SCIENCE CHINA
Physics, Mechanics & Astronomy

• Invited Review •

December 2015 Vol. 58 No. 12: 124701
doi: 10.1007/s11433-015-5745-9

On the instability of offshore foundations: theory and mechanism†

GAO FuPing[1*], LI JinHui[2], QI WenGang[1] & HU Cun[1]

[1] *Institute of Mechanics, Chinese Academy of Sciences, Beijing 100190, China;*
[2] *Centre for Offshore Foundation Systems, University of Western Australia, Perth WA 6009, Australia*

Received September 15, 2015; accepted October 10, 2015

As the offshore engineering moving from shallow to deep waters, the foundation types for fixed and floating platforms have been gradually evolving to minimize engineering costs and structural risks in the harsh offshore environments. Particular focus of this paper is on the foundation instability and its failure mechanisms as well as the relevant theory advances for the prevailing foundation types in both shallow and deep water depths. Piles, spudcans, gravity bases, suction caissons, and plate anchors are detailed in this paper. The failure phenomena and mechanisms for each type of foundations are identified and summarized, respectively. The theoretical approaches along with sophisticated empirical solutions for the bearing capacity problems are then presented. The major challenges are from flow-structure-soil coupling processes, rigorous constitutive modeling of cyclic behaviors of marine sediments, and the spatial variability of soil properties for large-spreading structures. Further researches are suggested to reveal the instability mechanisms for underpinning the evolution of offshore foundations.

failure mechanism, bearing capacity, fluid-structure interaction, offshore foundation, soil dynamics

PACS number(s): 81.05.Rm, 46.70.Lk, 91.50.Jc, 62.20.Fe

Citation: Gao F P, Li J H, Qi W G, et al. On the instability of offshore foundations: theory and mechanism. Sci China-Phys Mech Astron, 2015, 58: 124701, doi: 10.1007/s11433-015-5745-9

1 Introduction

Since the first offshore platform (oil rig "superior") for oil and gas exploitations was constructed in just 6.1 m depth of water in 1947, over 7000 offshore platforms worldwide are located from shallow to deep waters. Nowadays, the terms "deep water" and "ultra-deep water" for the offshore engineering are generally referred to around 500 m and 1500 m, respectively [1].

In shallow waters, the fixed platforms with concrete or steel legs installed directly on the seabed have been adopted for supporting a deck with space for drilling rigs or production facilities and crew quarters. The fixed platforms mainly include jacket platforms (jacket), jack-up mobile drilling rigs (jack-up), gravity-based structures (GBS). The increasing demanding for hydrocarbon has now led the offshore industries to the deeper water. Nevertheless, the cost of traditional fixed jacket platforms increases exponentially with water depth due to the expenses in the material and construction. As such, several types of floating structures have been developed for deep water applications, e.g. tension-leg platforms (TLP), spar platforms (spar), semi-submersibles, and floating production, storage, and offloading facilities (FPSO). Such floating structures are normally anchored to the seabed with catenary or (semi) taut mooring systems. With the increase of water depth, the dynamic interactions between floating platform and its mooring system become increasingly important [2].

In the harsh offshore environments, these engineering structures have occasionally been destroyed or damaged. For example, during hurricanes Katrina and Rita in 2005, about 109 offshore platforms (including 5 drilling rigs) were destroyed in the Gulf of Mexico. Around the world, about

*Corresponding author (email: fpgao@imech.ac.cn)
†Recommended by LI JiaChun (CAS Academician)

12% of the jack-up rigs experienced fatal incidents from 1970 to 2007 [3]. Field investigation showed that the instability of the foundation system is one of the main causes for destroy of whole structures. The instability of offshore infrastructures and even the upper units involves complex flow-interaction-soil coupling processes. Understanding and predicting physical mechanisms of structure-soil interactions under severe offshore loads are vital for the stability and safety of offshore engineering structures [4].

Along with the platform innovations during the offshore industry moving from shallow to deep waters, the foundations of offshore structures have undergone a steady evolution, aiming at providing bearing capacities to minimize engineering costs and structural risks. Initially, driven pile foundations were used in normally or lightly over-consolidated clays in the Gulf of Mexico with water depth of just 6 m. Gravity bases were then developed to adapt to the heavily over consolidated clays and dense sands in the North Sea. The gravity bases with skirts have been constructed in deeper water of up to 300 m. Suction caissons are an alternative type of foundation in North Sea due to the advantage of reduced installation time and material costs. In moderate water depth (up to 150 m), mobile jack-ups with 'spudcan' foundations are a key contributor around the world through their ability to self-install. The development in deep waters resulted in a variety of floating systems (e.g., FPSOs, semi-submersibles, TLPs, and spars) tethered with anchoring systems, such as suction anchors, plate anchors, and dynamically installed torpedo anchors.

In addition to the offshore oil and gas exploitations, offshore wind farms have also been developing rapidly. One of key features of offshore wind turbine structures is their relative light weight for the size level, yet they are subjected to large horizontal forces and overturning moments from the wind, waves and currents in shallow waters. The horizontal load may be of the order of 65% of the vertical load. The foundations for offshore wind turbines have their variety with some specificities, e.g. monopiles (widely used in Europe), high-rise multi-pile foundations (ever used in the East China Sea). In the offshore engineering for oil and gas, emphasis is mainly focused more on capacity (ultimate limit state) than on deformations (service limit state). However, with respect to offshore wind turbines, allowable deformation of the foundation is strict, making the deformation a critical concern in the design [5].

Historically, each type of the aforementioned offshore foundations was designed and constructed to endure certain hydrodynamics (waves, currents, tides), potential submarine geo-hazards and soil conditions of the seabed, e.g., soft clays, stiff sands, carbonate sediments and layered soils [6]. It has been well recognized that the more rapidly an industry or engineering technology is developing, the wider would be the gap between engineering practices (represented in design guidelines) and theory advances.

This paper aims to systematically summarize the foundation instability and its failure mechanisms as well as the relevant theory advances for the prevailing foundation types in both shallow and deep water depths. It is expected for understanding the difficulty and impossibility to cover all of the offshore foundation types due to space limit of the paper. Typical foundations for fixed structures (including piles, spudcans and gravity bases) are detailed in sect. 2. Typical ones for floating structures (including suction caissons, and plate anchors, dynamically penetrating anchors) are detailed in sect. 3.

2 Instability of foundations for fixed structures

2.1 Pile foundations: Conventional piles and monopile

Piles are a typical deep foundation composed of long, columnar elements made of steel or reinforced concrete. Pile foundations are commonly used in situations where the bearing capacity of the surface soils is insufficient to resist the imparted loads. Two different types of piles, i.e. driven steel piles and grouted piles, are prevalent at present. Driven piles are prefabricated off-site and much time can be saved for in-site installation, which makes it preferable in offshore applications.

Offshore piles are traditionally applied for supporting offshore platforms in relatively shallow water. Recently the large-diameter monopile is often used as the foundation of offshore wind turbines. The cost of transportation and installation of offshore piles is high and mainly depends on the design of piles. Hence, the precise evaluation of the pile response under severe offshore loading conditions caused by wave, current and wind are urgently needed. The axial and lateral pile responses will be detailed in this section.

2.1.1 Axial bearing capacity: progressive failure of long piles

The ultimate axial capacity of piles subjected to compression is composed of the shaft friction capacity and the end bearing capacity. According to the relative contribution from the two parts, vertically loaded piles are classified as end-bearing piles and friction piles. The unit shaft friction and unit end bearing can be evaluated from various formulations for both cohesive and cohesionless soils [7,8]. Under non-extreme conditions, the axial pile displacements are important for serviceability requirements, and can be commonly evaluated using a load transfer approach [9]. The load transfer curves in clay reach the peak shear stresses at a displacement of 1 percent of the pile diameter and decay beyond the peak by up to 30 percent due to strain softening. Progressive failure of long, compressible piles could occur due to the strain-softening of the load transfer response along the pile shaft. For a long and compressible pile, significant difference of pile displacements between the head of the pile and the toe of the pile would exist and thus the

peak shaft resistance can't be mobilized simultaneously along the whole pile, resulting in a smaller capacity comparing with that of the rigid pile [10]. A 'critical' pile length should exist beyond which the actual axial capacity would not be dependent on the pile length, due to the progressive failure of long piles.

For pile groups which are widely used in engineering practice, the bearing capacity of each single pile is reduced due to interaction effects. More work on the pile group effect can refer to ref. [11].

2.1.2 *Lateral pile response*

(1) Failure mechanisms of a long flexible pile

While evaluating the response of a laterally loaded pile, piles are usually categorized into long/flexible piles and short/rigid piles depending on the failure mechanisms. According to Poulos and Hull [12], piles having a length of $L_c/3<L<L_c$ are proposed as the transition range from flexible to rigid pile, in which L_c represents the critical pile length beyond which any further increase in length doesn't affect the pile head response. Figure 1 illustrates the lateral failure mechanism for long piles. In Figure 1, D denotes the pile diameter and e denotes the load eccentricity. For flexible piles, pile deflections and bending moments induced by the lateral loading are confined to the upper part of the pile and the pile embedment depth has insignificant effect on the pile response. It would be wasteful and pointless to adopt a pile embedment that is much larger than the critical pile length. The yield moment of the pile may be reached before full mobilization of the ultimate soil resistance.

While designing piles for resisting lateral and moment loading, the failure criterion is often the tolerable deflection of the piles rather than the ultimate lateral capacity. Therefore, the load-deflection behavior of laterally loaded piles has attracted much attention. For long piles, Hetenyi [13] derived the following linear solutions for the pile deflection u and rotation θ at the loading position of the laterally loaded piles based on subgrade reaction theory, which idealize the laterally loaded pile as an elastic beam transversely restrained by uniform, linear springs distributed along the pile length:

$$u=\sqrt{2}\frac{H}{k}\left(\frac{L_c}{4}\right)^{-1}+\frac{M}{k}\left(\frac{L_c}{4}\right)^{-2},$$

$$\theta=\frac{H}{k}\left(\frac{L_c}{4}\right)^{-2}+\sqrt{2}\frac{M}{k}\left(\frac{L_c}{4}\right)^{-3},$$

in which H denotes the horizontal loading, M denotes the moment applied to pile at ground level, k denotes the coefficient of subgrade reaction. The critical pile length here is expressed as $L_c\approx 4\left(E_pI_p/k\right)^{1/4}$, in which E_p denotes the elastic modulus and I_p denotes the second moment of area of a pile. From the simple idealization of subgrade reaction theory, several linear solutions for the load-deflection behavior of laterally loaded piles in the uniform soil and Gibson soil have been proposed based on the integral equation method [14] or the finite element analyses [15]. These solutions were proved to be in reasonable agreement.

Soils exhibit nonlinear stress-strain behavior even at very small strains [16]. The degradation of the soil stiffness with increasing soil displacement can be captured by idealizing the soil as a series of independent springs distributed along the pile length, with each spring describing the nonlinear relationship between the lateral soil resistance p, and the lateral deflection of the pile y. This is known as p-y method. Reese et al. [17] derived p-y curves in sand based on the full-scale tests at Mustang Island by adopting wedge failure mechanism at shallow depths and soil flow mechanism at deep depths to evaluate the ultimate lateral resistance p_u (see Figure 1). The gradient with depth of the initial stiffness of the p-y curves k_{ini} is determined according to the relative density/internal friction angle for the sands. The combined analysis resulted in semi-empirical p-y curves which consisted of four discrete parts assembled into a piecewise curve. Based on the piecewise p-y curves proposed by Reese et al. [17] and a relatively large database of laterally loaded pile tests, O'Neill and Murchison [18] suggested a modified p-y curve in sand:

$$p(y)=Ap_u\tanh\left(\frac{k_{ini}z}{Ap_u}y\right), \tag{1}$$

in which A is a coefficient for adjusting the value of p_u to guarantee a satisfactory agreement with the full-scale tests at Mustang Island. The hyperbolic tangent p-y curves in eq. (1) are currently incorporated into the design regulations [5,9].

The p-y curves in eq. (1) are significantly dependent on the soil internal friction angle ϕ', whilst the values of ϕ' are typically derived from the results of cone penetration tests. Therefore, it is attractive and logical to link the lateral soil

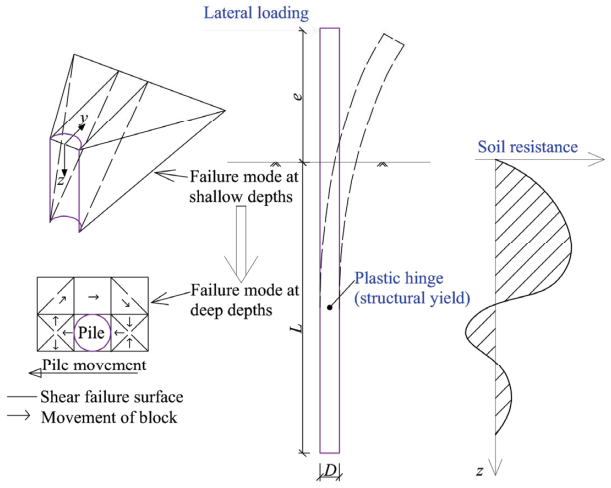

Figure 1 (Color online) Lateral failure mechanism for long/flexible piles.

resistance to the cone resistance q_c. Recently, a numerical study has been undertaken by Suryasentana and Lehane [19] to link the lateral soil resistance to the cone resistance q_c for silica sands. The *p*-*y* curves was expressed as:

$$\frac{p}{\sigma'_{v0}D}=2.4\left(\frac{q_c}{\sigma'_{v0}}\right)^{0.67}\left(\frac{z}{D}\right)^{0.75}\left\{1-\exp\left[-6.2\left(\frac{z}{D}\right)^{-1.2}\left(\frac{y}{D}\right)^{0.89}\right]\right\}, \quad (2)$$

in which σ'_{v0} is the *in-situ* vertical effective stress of the soil. The increase of the lateral soil resistance expressed with eq. (2) is rather gradual compared with the hyperbolic tangent relationship in eq. (1). Eq. (2) aims to cover the range of pile diameters from approximately 0.5 m to 5.0 m whilst the validity of eq. (2) was only confirmed by several field tests with pile diameters around 0.6 m.

(2) Failure mechanisms of a rigid monopile: "toe-kick" phenomenon

Short piles rotate as a whole and develop a "toe-kick" phenomenon under the lateral and moment loading (see Figure 2(a) [20]). The failure mechanism of a short pile is significantly different from that of a long pile (see Figure 1), which forms the basis of the method in the current design regulations. The recommended *p*-*y* curves in sand in the current design regulations (eq. (1)) are developed based on the limited in-site tests dataset consisting of flexible piles with diameters smaller than 1.22 m. In contrast, typical offshore monopile foundations behave rigidly due to their large bending stiffness and small slenderness ratio *L*/*D* [21]. The methods in the existing standards (eq. (1)) cannot be applied to the monopile foundations. The current *p*-*y* method should be calibrated for a short pile [22].

Figure 2(b) illustrates the mobilized soil resistance components of a laterally loaded short pile. Significant base shear and axial resistance are mobilized at the pile tip comparing with the flexible piles. Vertical side resistances emerge around the short pile shaft due to the relatively large horizontal displacement of the pile tip and rotation of the pile. Numerical investigations by Bekken [23] and Byrne et al. [24] showed that the contributions due to the horizontal pile tip displacement and rotation of the pile had significant effects on the lateral response of a short pile. To take the tip resistance and side resistance into account, three types of springs relating the resistance could be incorporated into the current *p*-*y* method, i.e. a base shear lateral spring associated with the lateral shear force at the pile tip, a base rotational spring associated with the moment produced by normal pressures on the pile base, and the rotational springs that distributed along the pile length associated with the moment produced by the vertical shear stresses on the shaft of the pile. The relationships for describing the behavior of base springs and rotational springs still need to be further examined. Some beneficial lessons may be learned from the analyses of laterally loaded rigid cassion foundations due to their similar resisting mechanisms [25].

2.1.3 *Flow-pile-soil interaction effects*

The instability process of offshore piles involves the interaction between the flow, pile and soils (see Figure 3). The safety of offshore piles in sand could be significantly compromised by waves/currents-induced scour due to the relatively large pile diameter and small slenderness ratio [26]. Understanding the transient and localized turbulence around the structures, especially in the shear flows [27], would be of benefit to the reveal of corresponding fluid-structure interaction mechanisms [28]. Scour reduces the pile embedment depth and increases the load eccentricity, inducing much larger deformations of the pile and changing the profiles of the lateral soil resistance.

Scour effects for laterally loaded piles in sand have not

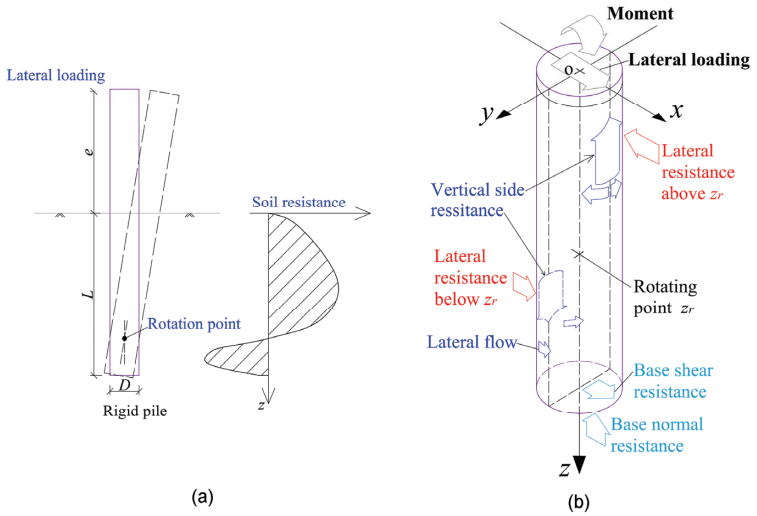

Figure 2 (Color online) (a) Lateral failure mechanism for short/rigid piles; (b) resistance components of a laterally loaded short/rigid pile (modified from Varun et al. [20]).

been well reflected in existing *p-y* method [9]. In an analytical study [29], general scour effects were incorporated by updating the parameters at a given depth to account for the over-consolidation induced by removal of a scour depth of sand. Lin et al. [30] further modified the lateral resistance due to changes in the shallow wedge-type failure mechanism to consider the effects of the local scour. Results indicated that the local scour hole would result in much higher lateral soil resistance for a given depth than for the general scour case, i.e. complete removal of the soil surface layer. Recently, a series of centrifuge tests were conducted by Qi [31] to investigate the scour effects on *p-y* curves. A practical approach to incorporate effects of scour on the *p-y* curves was proposed by adopting an effective soil depth (z_e) in the determination of *p-y* curves. The effective soil depth was expressed by

$$\frac{z_e}{D}=\frac{z'}{D}+\tanh\left(f\frac{z'}{D}\right)\frac{S}{D}\quad\begin{cases}f\approx 1.5 & \text{for local-scour,}\\ f=0 & \text{for general-scour,}\end{cases}\tag{3}$$

where the effective soil depth z_e is a weighted-average of the soil depth relative to the original mudline z and the soil depth below the current scour base z' (=z–S, S is the scour depth), f is an empirical parameter indicating the transition rate for the effective soil depth from $z_e = z'$ at the current mudline to $z_e \approx z$ as the soil depth increases. The recommended value of f=1.5 for local-scour conditions was based on the tests with 30° slope angle of the scour hole. For the cases with arbitrary slope angles, further investigations are needed.

Another important issue that should be considered for evaluating the behavior of the laterally loaded offshore piles is the effects of excess pore-pressure. For the soils around a pile foundation, excess pore-pressure could be induced by the action of waves [32] or the cyclic movement of piles [33]. The soil resistance around the pile might be changed significantly by the excess pore-pressure (see Figure 3). At present, no guidelines are available to account for the effects of wave-induced and cyclic pile movement-induced pore-pressure on the lateral pile response. A simplified *p*-multiplier method (the multiplier is dependent on the relative density of soils, and normally less than 1.0) was applied to the common *p-y* curves to evaluate the effects of seismic-induced liquefaction on the lateral pile response [34]. Such analysis method for the seismic loading can be employed for reference in the conditions of ocean wave loading and cyclic pile movement.

In addition, accumulation of foundation deformation induced by the cyclic loading would bring more challenges for deformation-sensitive structures, e.g. the fixed bases (conventional piles or monopiles) for wind turbines. As for piled foundations, the cyclic *p-y* curves in the current codes cannot consider the changes in the initial stiffness of the *p-y* curves induced by cyclic loading, with only the ultimate degraded resistance considered. Meanwhile, the limited number of load cycles (~100 load cycles) is another caveat of the cyclic *p-y* curves in the current codes, which has drawn much attention [21,35].

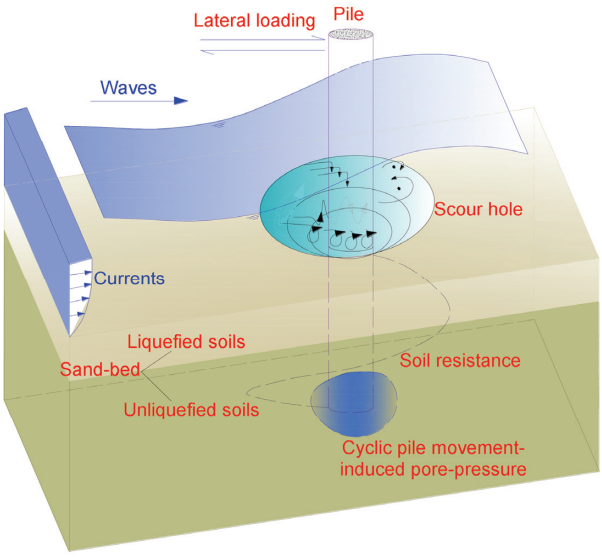

Figure 3 (Color online) Illustration of flow-pile-soil interaction.

2.2 Spudcans for jack-up platforms

A typical modern jack-up consists of a buoyant triangular hull, three independent truss-work legs and inverted conical spudcan foundations [36]. A jack-up is self-installed by lifting the hull from the water and pushing the large spudcans into the seabed. On location, the spudcan foundations are preloaded by pumping sea-water into ballast tanks in the hull. This preloading process tests the foundation to ensure enough bearing capacity during extreme storm events. The installation and preloading process is complex as the spudcan foundations penetrate into the seabed. Various failure mechanisms have been revealed for different soil conditions, mainly including bearing capacity failure in uniform soils, punch-through failure in layered soils and lateral squeezing failure on soft clays. During storms, the foundations are subjected to vertical loads, overturning moments as well as horizontal shearing loads. The capacity of the spudcans under combined loading needs to be carefully assessed. The problems of existing footprint, extraction of spudcans and skirted spudcan are not included in this review and can be found in recent publications [37–41].

2.2.1 Yield envelope for spudcan under combined loading

The offshore environmental loading condition on jack-up platforms often leads to large vertical (V), horizontal (H) and moment (M) loads being applied to the spudcan foundations. ISO [42] provided a yield interaction surface (envelope) to define the limiting combinations of the spudcan moment, vertical and horizontal reactions.

The yield envelope is a “rugby ball” shaped surface that

is elliptical in cross sections on planes at constant vertical load (V), and parabolic on any section including the V-axis (see Figure 4). This shape has been verified by the laboratory tests of spudcan foundations on clay by Martin and Houlsby [43]. This yield surface only accounts for the contribution from the underside of the spudcan while ignores the backflow at large embedment depths.

Zhang et al. [44] conducted centrifuge tests to characterize the yield surface in *VHM* space at various embedment depths and proposed a yield surface formulation as:

$$f=\left(\frac{H}{h_0V_0}\right)^2+\left(\frac{M/D}{m_0V_0}\right)^2-\frac{2eHM/D}{h_0m_0V_0^2}-\left[\frac{4}{(1+\chi)^2}\right]^2\left(\frac{V}{V_0}+\chi\right)^2\left(1-\frac{V}{V_0}\right)^2=0, \quad (4)$$

where V_0 represents the compressive vertical bearing capacity of the soil beneath the spudcan, h_0 and m_0 define the peak ratios of H/V_0 and M/DV_0 in the *VH* (M=0) and *VM* (H=0) planes, e defines the eccentricity of the cross section in the *HM* plane, and χ is the tensile capacity ratio V_t/V_0, V_t is the tensile capacity provided by the soil cohesive strength, D is the diameter of the spudcan.

The foundation behavior is considered elastic within the yield surface, which expands or contracts upon yielding according to a hardening law. The incremental plastic displacements at yield are described by a plastic potential. The size of the yield envelope is directly related to the vertical bearing capacity-plastic penetration curve. Figure 4 schematically illustrates the expansion of the *VHM* yield envelope with the penetration of the spudcan foundation [45] Provided the preload capacity of the jack-up is appropriate, the majority of the foundation load-deflection behaviour during a storm should be elastic (within the yield surface).

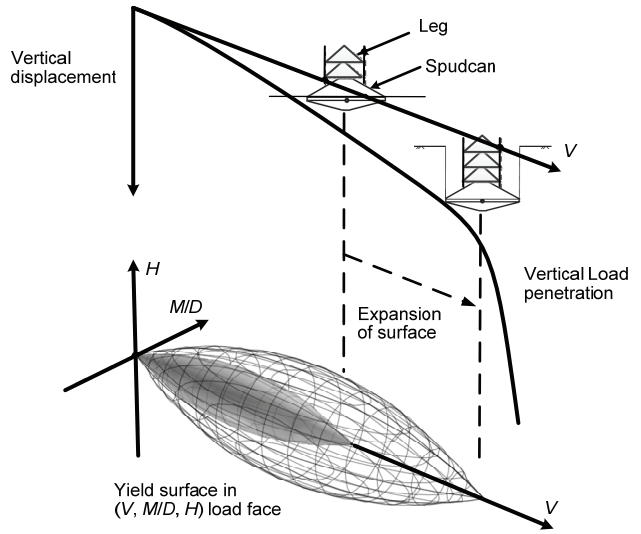

Figure 4 Expansion of the combined loading yield surface with spudcan penetration (after Randolph and Gourvenec [45]).

2.2.2 *Penetration of spudcans*

(1) Bearing capacity failure in uniform soil

Penetration of spudcan in clay is described by a load-penetration curve in ISO [42]. The bearing capacity of the foundation at different embedment depths is calculated using classical bearing capacity theory for wished-in-place footings at the corresponding depths. The gross vertical bearing capacity (Q_V) is calculated as:

$$Q_V=(s_uN_cs_cd_c+p_0')A_s, \quad (5)$$

where s_u is the design undrained shear strength of the clay, s_c and d_c are the shape factor and depth factor [46], p_0' is effective overburden pressure, A_s is the equivalent cross-sectional area of the spudcan, N_c is the bearing capacity factor. The recommended bearing capacity factor N_c is based on solutions for strip footing on homogeneous clay. An alternative bearing capacity factor accounting for the increasing undrained shear strength with depth was developed by Houlsby and Martin [47], which is also provided in Appendix E of ISO [42].

Hossain and Randolph [48] proposed a new design approach based on the observations on the failure mechanisms of spudcan penetration. As the spudcan penetration continues the soil failure transfers from a general shear failure at shallow depth to a full-localized failure at deep embedment with the soils beneath the spudcan flowing around until on the top of the foundation [49]. This approach is further extended to account for strain-rate dependency and strain softening [50]. These methods were assessed by comparing the predictions with the field measurements at 16 sites in the Gulf of Mexico [51,52]. The comparison indicates that the method by Houlsby and Martin [47] provides the lower bound load-penetration predictions. The Hossian et al. [49] method provides an upper bound load-penetration prediction. The ISO method [42] with Skempton factors provides reasonable predictions of the average penetration under a given load.

(2) Punch-through failure in layered soil

When a strong layer overlies a weak layer of soil, punch-through failure is of particular concern. A small additional penetration of spudcan can be associated with a significant reduction in bearing capacity, which leads to uncontrolled, rapid leg penetration (as shown in Figure 5). This process is particularly hazardous during installation of jack-up platforms.

The ISO [42] recommended using either a load spread approach or the punching shear mechanism to calculate the peak penetration resistance (q_{peak}) for a foundation on sand overlying clay. Both methods in the guideline were found to underpredict the peak resistance [53]. The reason lies in that the increasing bearing capacity of the foundation induced by a soil plug trapped below the spudcan is not accounted for in the guideline. A new calculation method accounting for the new failure mechanism was first proposed by Lee et al.

[54] and was further improved by Hu et al. [55]. The peak resistance is the sum of the frictional resistance in sand and the bearing capacity of the underlying clay (the first term in eq. (6)), as well as the weight of the trapped sand frustrum (the second term in eq. (6)):

$$q_{\text{peak}} = \left(N_{\text{c}} s_{\text{um}} + q_0 + 0.12\gamma' H_{\text{s}}\right)\left(1+\frac{1.76H_{\text{s}}}{D}\tan\psi\right)^{E} + \frac{\gamma' D}{2\tan\psi\left(E+1\right)}\left[1-\left(1-\frac{1.76H_{\text{s}}}{D}E\tan\psi\right)\cdot\left(1+\frac{1.76H_{\text{s}}}{D}\tan\psi\right)^{E}\right], \quad (6)$$

where s_{um} is the undrained shear strength at sand-clay interface, q_0 is the surcharge, γ' is the effective unit weight of soil, H_{s} is the sand thickness, D is the footing diameter, ψ is dilation angle, $E = 2\left[1+D_F\left(\tan\varphi^*/\tan\psi-1\right)\right]$, D_{F} is a distribution factor, ϕ^* is reduced friction angle due to the non-associated flow rule. The detailed interpretation of each parameter can be referred to Hu et al. [55]. More recent work on punch-through failure in sand-over-clay can be found in Qiu and Grabe [56] and Dean [57].

In regions of offshore South-East Asia problematic soil profiles with stiff stronger clay overlying weaker soft clay are increasingly encountered. ISO [42] recommended a punching shear method to predict the peak load of a spudcan under this soil condition. Edwards and Potts [58] proposed that the peak resistance was the sum of the bearing capacity of the underlying clay and a fraction of the capacity of the upper clay. It is found these predictions are significantly affected by ignoring the soil plug underneath the spudcan during penetration. Hossain and Randolph [48] proposed a new method based on centrifuge tests and large deformation finite element analysis with the peak resistance being a function of: (1) the strength ratio between lower and upper soil layers, $s_{\text{ubs}}/s_{\text{ut}}$; (2) the thickness of the upper layer relative to the spudcan diameter, t/D; (3) the strength gradient of the lower layer, k; (4) the relative roughness of the spudcan base. The formula of the peak resistance for a smooth spudcan in stiff-over-soft clay is written as:

$$\frac{q_{\text{peak}}}{s_{\text{ut}}} = 2.9Ln\left\{\left(\frac{s_{\text{ubs}}}{s_{\text{ut}}}\right)\left(\frac{t}{D}\right)\left(1+\frac{kD}{s_{\text{ubs}}}\right)\right\}+9.9. \quad (7)$$

(3) Lateral squeezing of soft clay

For a soft-over-strong clay system the failure mechanism of lateral squeezing of soft clay can occur. ISO [42] recommended the gross ultimate vertical bearing capacity proposed by Brown and Meyerhof [59] and Vesic [60] for a spudcan subjected to squeezing. The lower bound vertical capacity is given by general failure in the soft clay layer. The upper bound capacity is determined by the ultimate bearing capacity of the underlying strong soil layer. More work on the soil squeezing in multiple soil layers can be found in Merifield et al. [61] and Romos da Silva et al. [62].

2.3 Gravity bases

Gravity base is a typical shallow foundation usually constructed of reinforced concrete, often with tanks or cells which can be used to control the buoyancy of the finished gravity base. After construction in a dock, a gravity base is towed to its intended location and sunk to rest on the prepared surface of seabed. The tanks are often ballasted with

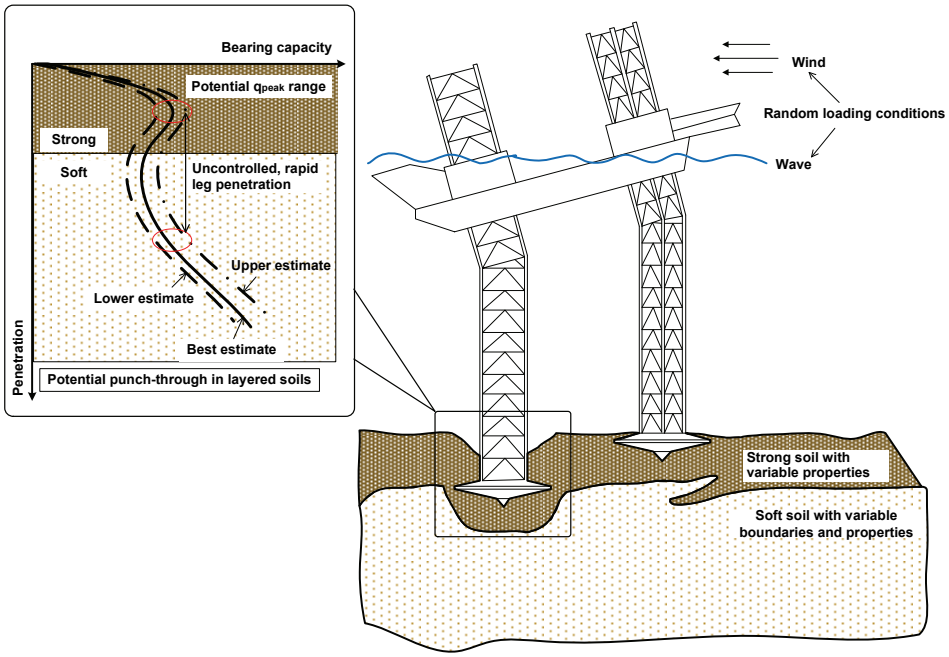

Figure 5 (Color online) Schematic of spudcan foundation showing potential punch-through in layered soils with variable boundaries and properties.

infill materials (e.g. sand, iron ore and rock) to increase the static weight of the gravity base and maintain its stability. If soft surficial deposits exist and incur challenges to withstanding the exerted loads, peripheral and probably internal skirts would be provided to penetrate into the seabed, confining the internal soil to displace rigidly and transmitting the foundation loads into deeper soil.

Historically, gravity bases have been widely employed in offshore oil platform and subsea installations (e.g. manifolds) since the first gravity-based platform Ekofisk I in 1973, and recently used for offshore wind turbines in water depths larger than 20 m [63]. A gravity base foundation holds in place and withstands the environmental loading by its weight, implying that the vertical static load is considerable and plays a key role in assessing its stability. Classical solutions for the vertical bearing capacity of shallow foundations are based on the original studies of a strip punch for plane-strain conditions done by Prandtl [64] and Terzaghi [65]. The interface between base bottom and the underlying soil was assumed to be smooth in Prandtl [64] and rough in Terzaghi [65], which makes the calculated bearing capacity of the former slightly smaller than the latter.

Interaction diagram and failure mechanisms for gravity base: In reality, gravity bases usually undergo combined vertical (V), moment (M), horizontal (H) and torsional (T) loading (i.e. fully three-dimensional loading), rather than purely vertical loading. Especially when utilized as foundations for offshore wind turbines, the vertical load resulted from the weight of turbines is relatively low compared to the significant horizontal and moment loads. The ratio of the moment to horizontal loading is generally an indication to determine the tendency between sliding and overturning failure. For a gravity base shallowly embedded in surficial sandy soil, the shear resistance between the base bottom and underlying soil is limited, making sliding resistance a critical issue in design. Conventional design approaches in API [9] adopt the modification factors to account for the interaction of horizontal and moment loading with vertical loading [66,67]. However, the effects of load inclination (i.e. *VH* loading) and load eccentricity (i.e. *VM* loading) are separately considered and conservatism arises for practical load combinations (i.e. *VHM* loading or general loading) from adopting the linear superposition of separate modifications for load inclination and eccentricity to represent the general loading [68]. Another conservative assumption of classical bearing capacity theory while applied to offshore design is that the approach neglects tensile capacity beneath the foundation, which is often significant for undrained conditions (clayey seabed or sandy seabed with the presence of skirts).

An alternative approach based on interaction diagrams or failure envelopes in *VHM* loading space [69] is become increasingly accepted to explicitly consider the interaction of these loading components. The failure envelope is a boundary to identify whether the foundation is safe under a certain combination of loads. The key advantages of the failure envelope approach over the conventional bearing capacity theory are explicit consideration of the independent loading components and a graphical interpretation of the factor of safety associated with different load paths [6].

Failure envelops for shallow foundations of various geometries (e.g. strip, circular and rectangular) have been derived using plasticity analysis and finite element analyses [68,70–73]. In these studies unlimited tensile strength was assumed for the interface (i.e. full-tension interface) between the base bottom and the soil, considering the fact that transient suction will prevent separation of the base bottom from the underlying soil for skirted foundations.

Different forms of upper-bound mechanisms composed of "scoop" mechanism and "wedge" mechanism were suggested. As shown in Figure 6, the Brinch Hansen mechanism [66] and Bransby-Randolph mechanism [70] are two representative plane strain mechanisms for strip loading under combined loading. In Figure 6(b), α and β represent the wedge angles and D is the width of the footing. A significant visual distinction between the two mechanisms is that the rotation centre of the "scoop" mechanism in the Bransby-Randolph mechanism locates above the soil surface while the rotation centre for the foundation and attached soil in the Brinch Hansen mechanism is below the soil surface. For the case of M=0, both mechanisms can degenerate to the asymmetric wedge of Green [74]. For the case with non-zero moment, the Brinch Hansen mechanism is optimal for high vertical loads, whereas Bransby-Randolph mechanism is optimal for low vertical loads [71]. For the case of V=0, reducing the horizontal loading and in-

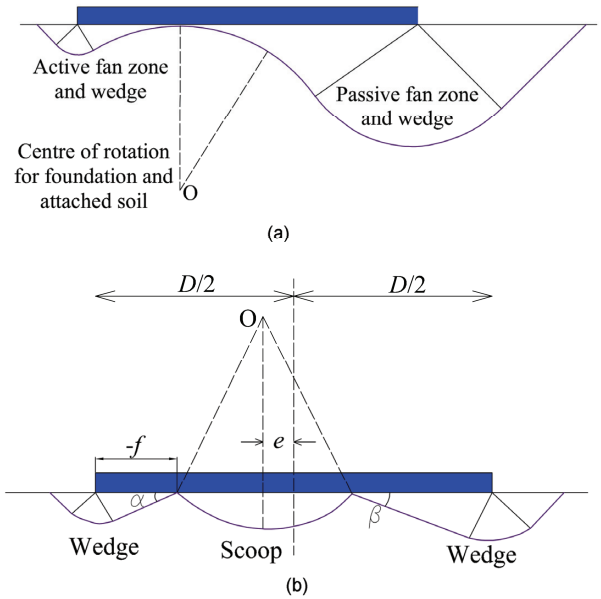

Figure 6 (Color online) Plane strain mechanisms for strip footing under combined loading: (a) Brinch Hansen mechanism; (b) Bransby-Randolph "wedge-scoop-wedge" mechanism (adapted from Randolph and Puzrin [71]).

creasing the moment loading would bring the rotation point above the foundation base, making the Bransby-Randolph mechanism prior to the Brinch Hansen mechanism [75]. This variation of mechanism with relative intensities of the horizontal and moment loading can be easily comprehended by comparing the two particular cases with purely horizontal loading (V=M=0, sliding failure) and purely moment loading (V=H=0, overturning failure).

The locus of the failure envelope in the *H-M* plane is found to be non-symmetric with the maximum moment sustained with a positive horizontal load [70,72]. This eccentricity of yield locus in *H-M* plane implies a strong nonlinear interaction between the loading components. Taiebat and Carter [72] found that the position of the maximum moment in *H-M* plane shifts towards the moment axis with increasing vertical loading. In practical engineering, foundations could be shallowly embedded in non-uniform soils and the corresponding failure envelopes were presented by Bransby and Randolph [76] for strip foundations and Vulpe et al. [73] for circular foundations, to account for the embedment ratio and soil strength heterogeneity. The thin surficial crust which arises in many deep-water locations could affect the failure envelope much. The effect of crust thickness has recently been taken into consideration by Feng et al. [77]. Feng et al. [78] also extended the failure envelope in *VHM* loading space to *VHMT* loading space to account for the effects of torsional loading.

The interface tensile strength between the base bottom and the soil is a key issue while deriving the failure envelope. Its effect has been evaluated by comparison between the "no-tension" case and "full-tension" case [75]. The failure envelope for "no-tension" case is attached to one corner of the larger failure envelope for "full-tension" case. The former is more symmetrical than the latter.

For drained conditions, the term yield envelope rather than failure envelope is commonly adopted. The general form of the yield envelope for a typical shallow foundation is a parabolic ellipsoid [79], similar to that for spudcans (see sect. 2.2.1). The yield envelope expands due to the occurrence of work hardening when the footing penetrates into the soil. More information on the detailed description of the yield envelope for shallow foundations and its expansion (hardening law) could be found in Houlsby and Cassidy [80] and Govoni et al. [81].

Scour effect: Loss of contact between base bottom and soil can occur due to scour induced by waves and currents. For the gravity base, scour is expected to be unacceptable due to their high reliance on the surficial soil, although this can be mitigated with skirts. Scour (up to ~3 m deep) around a gravity base has been reported by several researchers [82,83]. It is essential to evaluate the possible development of scour as an important input parameter for the skirt design [84].

3 Bearing capacity of foundations for floating structures

3.1 Suction caissons

A suction caisson, also referred to as "suction anchor", "skirt foundation", "suction pile" or 'bucket foundation", is usually a large diameter thin-walled cylindrical steel structure, which can visually be described as an upturned bucket (open-ended at the bottom and closed at the top installed with a vent valve) embedded in the marine sediment. The concept of "suction" technology was developed where gravity loading is not sufficient for pressing foundation skirts into the seabed. The diameters for suction caissons are typically in the range of 3–8 m. The length-to-diameter ratios of suction caissons range from 1.0 to 6.0, compared to typical ratios of 30–60 for traditional piles.

Since firstly installed for the foundation of the Floating Storage and Offloading unit (FSO) at the Gorm field in the North Sea in 1981, suction caissons have been increasingly used as anchors for floating structures in the offshore oil and gas industry, and have recently been proposed for use in conjunction with offshore wind turbines, etc. In South China Sea, suction caissons were used for the foundations of FPSOs at Wen-chang field (water depth: 120 m) in 2002, and Pan-yu field (water depth: 105 m) in 2003, respectively. Statistics in 2002 revealed that 485 suction caissons had been installed in more than 50 different localities around the world, in depths to about 2000 m [85].

3.1.1 Suction caisson installation: internal soil plug failure

During the installation process, an initial tip penetration is achieved under its submerged weight to provide a seal between the caisson and the underlying soil. Then a differential pressure ("suction") is generated by pumping water inside to bring the suction caisson further penetrating into the seabed (see Figure 7). After installation, the caisson's interior is sealed off and the vertical loading can create an internal excessive under-pressure ("suction"), which in turn mobilizes anti-tension bearing capacity. Several ring stiffeners are usually installed along the inner side of the caisson, which may effectively prevent the structural buckling during installation and due to the mooring loads and lateral soil resistance during operation.

The internal soil plug failure is the main concern for the installation of suction caissons. If a critical under-pressure is exceeded, soil heave would be induced and the caisson could not be penetrated deeper to the target depth. The critical under-pressure $\Delta u_{\mathrm{a}}\,\Delta u_{\mathrm{a}}$ is the maximum applied pressure without causing large soil heave within the caisson, which can be expressed as:

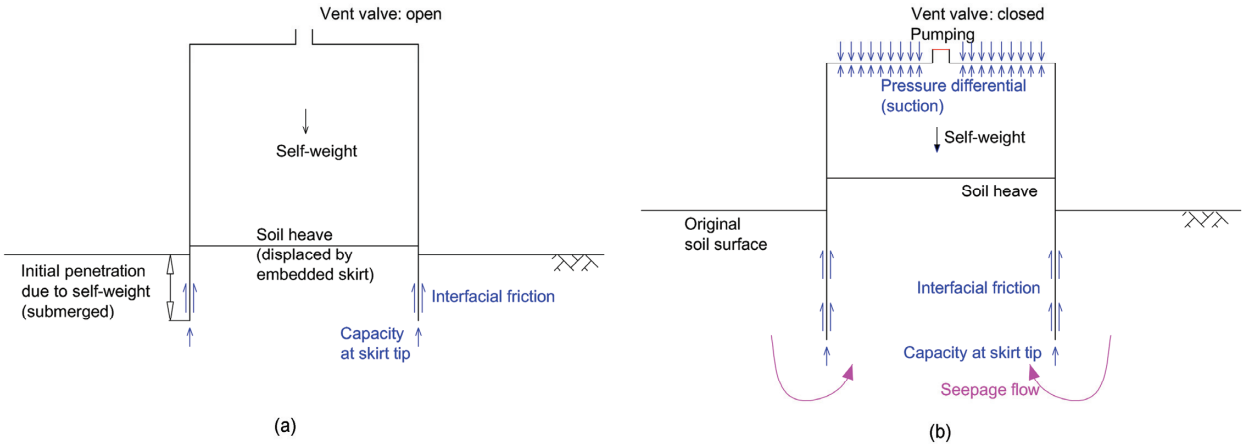

Figure 7 (Color online) Illustration of suction caisson installation: (a) stage-I: self-weight penetration, (b) stage-II: suction-induced penetration.

$$\Delta u_{\mathrm{a}}=\frac{A_{\mathrm{i}}N_{\mathrm{c}}s_{\mathrm{u\text{-}tip}}+A_{\mathrm{si}}\eta\overline{s}_{\mathrm{u}}}{A_{\mathrm{i}}}, \tag{8}$$

where A_{i} is the internal cross-sectional area of the caisson, $s_{\mathrm{u\text{-}tip}}$ is the undrained shear strength at skirt tip level, A_{si} is the internal skirt wall surface area, η is the adhesion or interfacial friction factor, $\overline{s}_{\mathrm{u}}$ is the average shear strength over penetration depth. The bearing capacity factor N_{c} varies from 6.2 to 9.0 with increasing the depth/diameter ratio. For a successful installation, the value of critical under-pressure to induce internal soil plug failure (Δu_{a}) should be larger than the necessary under-pressure (Δu_{req}) to penetrate the caisson into the soil:

$$\Delta u_{\mathrm{req}}=\left[A_{\mathrm{s}}\eta\overline{s}_{\mathrm{u}}+A_{\mathrm{tip}}\left(N_{\mathrm{c}}s_{\mathrm{u\text{-}tip}}+\gamma' z\right)-W'\right]\Big/A_{\mathrm{i}}, \tag{9}$$

in which A_{s} is the sum of the internal and external skirt-wall surface area, A_{tip} is the skirt tip area, W' is the submerged weight of the suction caisson [45]. Besides the soil properties (e.g. effective unit weight, shear strength, and soil heterogeneity) and interfacial frictions, the aspect ratio (length-to-diameter ratio L/D) is a key influential factor for the internal soil plug failure. For a typical normally consolidated clayey soil in deep waters, the internal soil plug failure is easier to occur for small aspect ratios, especially during the early installation stage.

Suction induced caisson-soil interaction during installation is more complex than aforementioned analyses. In sands under drained conditions, the exterior downward seepage increases the local effective stresses; by contrast, the interior upward seepage reduces the effective stresses of the sands inside the caisson, which may result in the seepage failures (quicksand, or piping). In clays, the caisson installation is generally under undrained conditions: the pressures within the caisson decrease sharply and those outside the caisson are usually little affected. The soil flowing into the caisson from its tip may not only fully around ring stiffeners, but also trends to extrude as a self-supporting inner plug [86].

If layered soils are encountered, especially ones containing dense sands or stiff clays, the penetration would be more difficult than that with homogeneous soils. In the engineering practice, the internal soil plug may be mitigated by reduction of the inner soil grains with the dredging-pump technique [87].

3.1.2 Vertical uplift capacity under undrained and drained conditions

The suction caisson technology functions very well in a seabed with soft clays or other low strength sediments, meanwhile it has also been employed in a sandy seabed. The soil drainage has much effect on the uplift bearing capacity of suction caissons. Whether perfectly/fully drained, partially drained or undrained behavior occurs is relative to the combined effects of bucket geometry, pull-out rate, soil permeability and soil strength [88].

Several semi-empirical failure models have been proposed for the vertical pullout of the suction caisson, e.g. model-A (undrained): reverse end bearing with passive suction, model-B (fully drained): only caisson pullout without passive suction, and model-C: caisson and internal-plug pullout without passive suction, etc. [89]. That is, the vertical uplift capacity sketchily comprises the submerged weight of the caisson, and (or) internal and/or external frictional resistance along the caisson shaft, and (or) reverse end bearing at the base of the caisson.

Undrained pullout capacity: During undrained (fully or partially) pullout in a silty or clayey seabed with low permeability under either monotonic or cyclic loading, negative pore-water pressures (passive suction) can be developed within the caisson. Meanwhile, the negative pressures may also result in the soil plug being retained within the caisson during the pullout process. As such, the undrained uplift capacity is generally larger than the drained capacity. For a fully undrained condition, the pullout capacity (V_{ult}) can be evaluated with the aforementioned semi-empirical failure

model-A, i.e.

$$V_{ult}=W'+A_{se}\alpha_e\overline{s}_{u(t)}+N_{cR}s_{u\text{-}tip}A_e, \quad (10)$$

where A_{se} is the external skirt wall surface area, A_e is the external cross-section area, α_e is the external adhesion or steel-soil interfacial friction factor, $\overline{s}_{u(t)}$ is the average undrained soil shear strength over penetration depth at time t after installation, N_{cR} is the reverse end bearing capacity factor (N_{cR} is normally around 9.0 or less), which is dependent on the mobilization of sufficient passive suction. If the vent valve is opened, or a sustained load is applied, the value of N_{cR} would be either not relevant or be reduced [45].

Drained pullout capacity: Drain tension/pullout capacity is particularly vital for the design of bucket foundations in a sandy seabed. For sandy soils in shallow waters, the aspect ratios of the caisson structure (*L*/*D*) are usually less than those in clayey seabed. Larger aspect ratios are favorable in particular for higher drained pullout capacity. However the penetration resistance increases greatly with embedment depth and the required suction is limited by the potential seepage failure as mentioned in sect. 3.1.1.

The state of the art for the physical modeling of the behaviors of suction caissons in sands under vertical tensile loads was recently summarized [88]. Since 1990's, physical tests have been preferably employed for understanding the drained responses and tensile capacity of the caisson in sands, including centrifuge tests, field tests or trials, small-scale tests (using silicon oil instead of water as the pore liquid phase) and scaling effect study. It was shown that the tensile capacity of the model bucket was strongly increased with the increase of pullout rate (0.03–0.56 times of the skirt length per second) as well as the decrease of sand permeability.

In addition to the aforementioned applications for floating structures in deep waters, the bucket foundations (monopod or multipod) have also been employed for fixed jacket structures early 1990's and recently for offshore wind turbines. Compared with a traditional monopile solution (see sect. 2.1), the bucket foundation design may reduce the steel weight by approximately half, and the installation is much easier, which does not require heavy installation equipment. Due to the relative light structure, the jacket structure with bucket foundations for the wind turbines is more likely to suffer a two-way (both tension and compression) cyclic loading in the offshore environments.

An adequate numerical modeling of the sand behavior around the suction caisson is still challenging due to the complex stress situation and the effects of dilatancy and densification on the effective stresses and the coupled pore pressure responses. To this aim, a coupled pore fluid diffusion and effective stress analysis was recently made by Thieken et al. [88], which is capable of describing the partly drained load-bearing behavior as well as the quantification of the tensile resistance. It was also indicated that a high pull-out rate leads to a large increase of the tensile capacity. The mobilization of suction pressures requires a large heave of the bucket, which might be inadmissible with respect to serviceability.

During the mobilization of the pullout capacity, the sand around the suction caissons can be liquefied due to suction-induced seepage forces. Rheologically, the shear strength and suction contributing to caisson capacity are dependent on shear strain rate associate with the pullout process. A Bingham plastic flow model was proposed to describe the shear stresses as a function of shear strain rate [90], which may provide an approach for estimation of the pullout capacity values corresponding to large displacement levels. It was assumed that ignoring liquefaction and sand flow could yield an overestimate of pullout capacity as a function of the induced deformation.

3.1.3 Bearing capacity under quasi-horizontal and inclined loading

Suction caissons were initially used as anchors for catenary moorings, where the chain angle at the padeye (located at the caisson side) is typically 10°–20° and the angle at the seabed surface approaches zero. With increasing water depth, the weight of a catenary mooring line becomes a limiting factor, which has to be overcome by using light synthetic rope and taut (or semi-taut) mooring. The taut mooring line is capable of resisting both horizontal and vertical loads, i.e. inclined loads with an angle of 30°–50° to the horizontal.

Horizontal bearing capacity of a suction caisson is maximized by positioning the padeye with an optimal position (downward) around 0.65–0.70 of the embedded caisson length, such that the caisson translates at failure without rotating [85]. The failure modes of suction caissons loaded horizontally and inclined at the seabed are similar to those for laterally loaded piles, which can be referenced in sect. 2.1.2.

The inclined bearing capacity of a suction caisson depends greatly on whether a crack develops along the trailing edge of the caisson. As such, positioning the padeye was suggested just below the optional depth to ensure backward rotation at failure, thereby reducing the potential for a crack to open on the trailing edge of the caissons [91].

During the failure process under inclined loads, significant vertical movement may occur. The maximum horizontal and the vertical components of the load at failure will be less than the respective capacities in the two extreme loading directions [92]. For the general inclined loading condition, the interaction between vertical and horizontal loading can be modeled by developing a special failure envelope in the VH loading plane, which is similar with the Spudcan detailed in sect. 2.2.

3.2 Plate anchors

Besides the aforementioned suction anchors, plate anchors

are alternative solution for deep water mooring systems. Plate anchors mainly comprise of a broad steel plate (fluke), a rigid shank and anchor chains, which are more attractive economically for the ease of fabrication and emplacement than suction anchors.

Typical plate anchors include drag embedment anchor (DEA), vertically loaded anchor (VLA) and suction embedded plate anchor (SEPLA). DEAs and VLAs are penetrated into the seabed with the drag of anchor handling vessels, while a SEPLA is positioned into the seabed by suction caisson (Figure 8). VLAs are installed like a traditional fixed fluke anchor (DEA) by applying a horizontal load at the mudline to achieve embedment. Due to improved geometry design, VLAs can be installed with deeper embedment than DEAs, to depths of up to 7–10 times of the fluke length (the typical fluke length of a VLA is up to 6 m). Till now, DEAs have been widely used in the catenary mooring systems to resist quasi-horizontal loads [93]. In China, the first deepwater drilling platform (CNOOC 981) has been equipped with DEAs, in addition to the dynamic positioning system. SEPLAs and VLAs are preferably employed to resist loads with large vertical components for taut or semi-taut mooring.

3.2.1 Kinematic trajectory of drag anchors and embedment depth loss of SEPLAs

The stability of floating facilities is not as sensitive as the fixed platforms to the foundation displacement or deformation. As such, the bearing capacity is the dominant factor in the design for deepwater foundations rather than the allowable displacement.

The bearing capacity of plate anchors largely depends on the final embedment depth. Prediction of the kinematic trajectory and the final embedment depth is the main concern for DEAs and VLAs [94]. As the anchor is dragged into the soil from the seabed surface, the chain continuously cuts through the neighboring soil and finally forms an inverse-catenary shape due to the soil resistance. In turn, the development of the inverse-catenary shape increases the loading angle at the padeye, which makes the plate rotate to the horizontal direction and eventually prevents further embedding into the seabed [45,95]. By assuming the anchor moves approximately parallel to the plate, the limit equilibrium analysis in combined with the inverse-catenary chain solutions was performed to obtain the final embedment depth [94]. The kinematic incremental approach has currently been used for the trajectory simulation, in which the continuous embedment process is modelled with the development of yield envelops.

In contrast to the uncertainty in the embedment depth of a DEA, a SEPLA is embedded into a target depth with the assistance of a suction caisson, with the plate being in a vertical orientation after the initial penetration. To effectively resist the loads, the anchor plate must be rotated from the previous vertical orientation to an inclined angle, i.e. the anchor plate is approximately normal to the mooring line. This process is known as “keying”, which usually causes the loss of the embedment depth (typical in the range of 0.5–1.5 fluke width) [6]. As the seabed sediment, e.g. the normally consolidated clay, typically exhibits lower shear strength in shallower depth, the embedment depth loss would essentially reduce the bearing capacity.

During the keying process, the plate anchor is subjected to a combination of shear, normal and moment loading. A plasticity model based on the failure envelop was used to assess the keying of plate anchors [96]. It was found that during the initial keying, the shear and moments dominate the rotation of the plate anchor. As the keying continues, the shear component decreases and the normal component increases monotonically, while the moment increases initially and then decreases. Influential factors for the embedment loss were investigated using large deformation finite element analysis validated with the experimental data [97]. Based on the parametric analyses, the following empirical relationship was established with non-dimensional forms for predicting the loss of embedment:

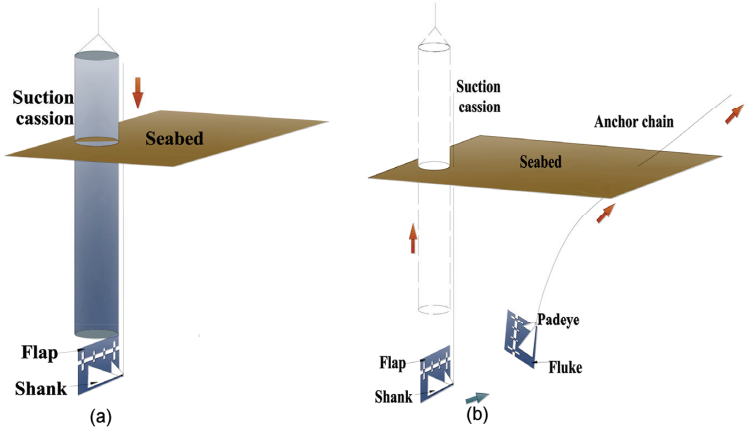

Figure 8 Installation of a SEPLA: (a) initial penetration; (b) keying process.

$$\frac{\Delta_{\text{depth}}}{B_{\text{e}}} = a_{\text{e}}\left[\left(\frac{e_{\text{e}}}{B_{\text{e}}}\right)\left(\frac{t_{\text{e}}}{B_{\text{e}}}\right)^{p_{\text{e}}}\right]^{q_{\text{e}}} \tanh\left[b_{\text{e}}\left(\frac{s_{\text{u0}}}{\gamma'_{\text{a}}\sqrt{t_{\text{e}}e_{\text{e}}}}\right)^{r_{\text{e}}}\right], \quad (11)$$

where Δ_{depth} is the embedment loss, e_{e} is the load eccentricity (perpendicular distance of the padeye from the anchor plate), t_{e} is the thickness of the anchor plate, s_{u0} is the local soil strength at the initial embedment depth of the anchor, γ'_{a} is the submerged unit weight of the steel anchor, the five empirical coefficients are fitted as a_{e}=0.144, b_{e}=5, p_{e}=0.2, q_{e}=−1.15, r_{e}=8.

A keying flap has been incorporated in current design of a SEPLA, aiming to reduce the embedment loss. It was noticed that, unlike expected, the flap did not rotate during the keying process but rotated at the end of the keying. The shearing force was balanced by the soil bearing pressure at the back of the flap during the keying process [98]. However, the presence of the flap was beneficial to reduce the loss of embedment due to padeye offset to the center of the whole anchor [99]. In general, the padeye offset has a positive effect on improving the bearing capacity. But with increasing in the padeye offset, the anchor would rotate beyond the normal to the mooring chain, further reducing the bearing capacity. Therefore, in the design of SEPLAs, the two compensating effects of padeye offset on the capacity should be well balanced.

3.2.2 Quasi-static pullout capacity

The quasi-static pullout capacity of a plate anchor usually increases with embedment depth and approached a constant value. This transition occurred at a critical ratio of the embedment depth to the width of the plate anchor, where a "localized flow-around" mechanism occurs under the deeply embedded conditions [100]. For a shallowly embedded anchor, the shear plane may extend from the anchor edge upward to the seabed surface, i.e. a general failure occurs [101].

The accurate prediction of holding capacity for a DEA or a SEPLA depends on the ability to effectively simulate the installation process. The whole holding capacity of such anchoring foundation (chain tension at the mudline) is comprises of both the ultimate tension in the anchor line at the padeye (T_{a}) and the distributed friction forces along embedded anchor line (arising from the submerged self-weight of the chain, whose effect is significant at shallow embedment depths). For a VLA and a SEPLA, the loading direction is approximately normal to the anchor plate. As such, the ultimate tension at padeye (T_{a}) can be evaluated with the traditional bearing capacity theory [102]:

$$T_{\text{a}} = A_{\text{f}} N_{\text{c}} s_{\text{u}}, \quad (12)$$

where A_{f} is the fluke bearing area, s_{u} is the undrained shear strength at the fluke level. The bearing capacity factor N_{c} here is typically taken in the range of 12–13, for the deeply embedment "localized flow around" failure mechanism. The value of N_{c} is influenced by the embedment depth ratio, the strength and stiffness of the soil, and the roughness of the plate anchor [101].

When the plate anchor is used for permanent mooring, its surrounding soil will be under fully or partially drained conditions. The long-term (drained) performance of the plate anchor against sustained uplifts would be significant. The undrained pullout capacity comprises three components, i.e. the net ultimate capacity, the effective self-weight and the suction force (typically around 20%–74% of the total capacity) [100,103]. The suction around the plate anchor prevents the soil separating from the plate during pullout, inducing a larger capacity than the breakaway situation. Under the long-term uplifts, the suction would gradually disappear with the dissipation of the pore pressure. Meanwhile, the anchor displacement can be accumulated during the consolidation process [104–106]. When the anchor displacement reaches a critical value, the consolidation underneath the anchor would be faster than above the anchor, resulting in the anchor breakaway from the soil. The sustained capacity of the pate anchor can be significantly lower than predicted with eq. (12) [107].

3.2.3 Cyclic pullout capacity

Under ocean waves and current in the offshore fields, the hydrodynamic loads transmitted form the floating structures to the plate anchors through mooring lines always remain in tension. This implies that the plate anchors are subjected to one-way cyclic loading (without stress reversal). Compared to two-way cyclic loads, one-way cyclic loads cause less degradation both in the shear strength and stiffness of the soil. One-way cycling was previously considered to have limited negative/detrimental effect on the cyclic pullout capacity, the reduction of which could be compensated by increasing shear strength of the soil in front of the anchor due to the consolidation under the sustained loading. Nevertheless, recent experimental test results indicated that there exists a threshold of cyclic loading (fraction of the pullout capacity), beyond which the plate anchor may experience failure due to large displacement and stiffness degradation of the plate-soil interaction system [104,108,109].

Current assessment of the cyclic pullout capacity of plate anchors was based on the steady limit equilibrium approach proposed for the cyclic response of gravity foundations [110], in which the degradation in the soil bearing capacity was depicted using the cyclic triaxial and direct simple shear strength of the typical soil elements along the potential failure surface. Obviously, the semi-empirical approach could not take into account the effects of the pore pressure accumulation and the stiffness evolvement.

Accurate prediction of the cyclic pullout capacity for plate anchors with numerical simulations largely depends on the constitutive models, which is capable of efficiently describing the predominant behaviors of the soils under

cyclic loading. At least two remarkable types of models have been developed for cyclic behaviors of soils. One type is the visco-elasticity models based on Masing's rule, which could capture the softening of the stress-strain but hardly consider the pore pressure generation and the accumulation of the plastic strain. The other type is the elasto-plasticity models, mainly including multi-surface (MS) models, and bounding surface (BS) models. The MS model contains infinite yield surfaces, which hardens in the stress space according to kinematic rules. In practice, the BS model can be considered as a special MS model, which contains a bounding and a yield surface. Both types of models can predict the hysteresis properties, the accumulated plastic strain and the evolvement of the stiffness of soils. The BS model was adopted to simulate the soil in the cyclic pullout analysis on the plate anchor [111], in which the threshold for cyclic loading induced failure was identified numerically. Under one-way cyclic loading, if the cyclic loading component is beyond the threshold value, significant degradation of soil shear strength may be induced within several loading cycles.

3.3 Dynamically penetrating anchors

The cost of installing anchors increases exponentially as water depths increase, which has inspired the development of dynamically penetrating anchors that embed themselves into the seabed under free-fall and thus are less sensitive to increasing water depth compared to conventional concepts [112,113]. Dynamically penetrating anchors or termed as Gravity-installed anchors are usually released from a height of 50–100 m above the seabed and reach velocities of 20–30 m/s at the seabed, eventually installed to the tip penetration of 1.5–3 times their length. The anchor is typically 10–17 m in length and 80–100 tons in weight. Due to different shapes, the dynamically penetrating anchor can be divided into torpedo anchor with four fins at the trailing edge (the initial use was at the Compos Basin), the deep penetration anchor (DPA) which has been installed in North Sea recently and OMNI-Max anchor.

During the penetrating process, the kinematic performance of the anchor will depend on the end bearing resistance, the shearing force and the inertial drag force. Due to the high penetration velocity, the strain rate effect at the soil-anchor interface is significant. When subjected to an inclined load transmitted by the mooring line, the anchor chain would slide through the soil and the orientation of the anchor would be adjusted. Challenges associated with dynamically penetrating anchors include prediction of the anchor embedment depth and the subsequent capacity.

4 Concluding remarks

The instability mechanisms and the relevant theoretical approaches for the prevailing foundation types in both shallow and deep water depths have been identified intensively and summarized systematically. Pile foundations, spudcans, gravity bases, suction caissons, plate anchors and dynamically penetrating anchors are detailed, respectively, indicating the failure mechanisms for offshore foundations are of wide diversity and some of them have not been well revealed.

With the offshore oil and gas exploitation moving into deep waters, the extreme environmental conditions will be encountered. The offshore foundations will be increasingly exposed to a large range of submarine geo-hazards, e.g. submarine slides, steep and rugged terrain at continental slopes, migrations of gases through the shallow stratum, even interactions of the seabed or subsea structures with internal solitary waves [114]. By contrast, in the nearshore wind farms in shallow waters, the hydrodynamics and aerodynamics on the wind turbine are equally prevailing on the structural and foundation responses.

The major challenges for offshore foundation instability are detailed as follows.

(1) Flow-structure-soil coupling processes

Failure mechanisms under severe offshore environmental conditions are still great concerns. The primary loads on offshore structures are wind, waves, currents and tidal loads, which exert cyclic loading on not only seabed, but also foundations and platforms. The coupling or interaction between flows, structures and soils is one of the essential features for the dynamic responses of offshore foundations. As an indicator of the flow-structure-soil coupling effect, soil scour around submarine structures/foundations may wash away a large amounts of sediments and further reduce the bearing capacity significantly. As such, soil scour (general and local scour) should be taken into account when evaluating the foundation instability [31]. In the shallow waters, the waves and currents are always coexisting; the wave-induced soil liquefaction [115] would be coupled with the local scouring process, which further complicates the failure mechanism of foundations.

Similarity theory combining with small-scale tests have been adopted for analyzing the complex flow-structure-soil coupling problems. Scale effects need to be carefully examined and be verified by field observations, or large-scale experiments. Moreover, a multi-discipline based structural optimization would be functional for the design of offshore foundation systems.

(2) Rigorous constitutive modeling of cyclic responses

Current analyses on the ultimate bearing capacity are mainly within the framework of conventional plasticity theories along with sophisticated empirical solutions. Despite great developments achieved on the elasto-plastic constitutive modeling, there are still challenging issues in understanding the macroscopic behaviors of granular materials [116]. Advanced constitutive models have not been efficiently used for reveal the complex failure mechanism, es-

pecially for the cyclic behaviors of marine sediments, e.g. seabed liquefaction, the structure/foundation-soil interactions under the cyclic loading.

The dominant soil behaviours under cyclic loading include hysteresis, degradations of shear strength and stiffness as well as the accompanying accumulation of plastic strain and excessive pore pressure. The constitutive models that describe/capture all these behaviours would be too lengthy and complicated to be used effectively. An applicable constitutive model that is efficient and robust in numerical implementations for accurate prediction of cyclic responses is needed.

(3) Spatial variability of soil properties for large- spreading structures

For a typical mooring system in deep waters, the engineering activity extends over a wide area, e.g. several tens of square kilometers or more. *In-situ* geotechnical investigations in deep water are extremely expensive, which limits the number of borings. As such, the uncertainties in the soil properties, soil stratification, loading conditions as well as the prediction models are considerable and the spatial variability effects should be carefully assessed.

How to incorporate these uncertainties into the geotechnical design in a systematic manner needs to be explored intensively. A single load-displacement curve of foundations obtained using deterministic models cannot accommodate the well-acknowledged uncertainties. If the observed response deviates from the prediction (as inevitably it will), how is the user to determine whether this deviation has significance or not? A range of the load-displacement curves considering the variation of the soils can achieve improved understanding and provide a basis for the inclusion of the monitored data into decision-making [117]. Even for gravity bases and spudcans subjected combined loadings, a deterministic yield surface still risk the foundations to fatally fail due to ignoring the uncertainties in the soil properties and loadings [118]. The yield surface or failure envelope is better to be expressed in terms of confidence intervals of *VHM* failure envelope. The probabilistic models are capable of providing additional information on assessing how reliable the deterministic prediction is, leading to a safer installation and operation of the foundations.

New challenges would be incessantly emerging with the rapid development of offshore engineering practices. Scientific reveal of instability mechanisms and advancing relevant theories would underpin the evolution of offshore foundations.

This work was supported by the National Natural Science Foundation of China (Grant Nos. 11232012, 11372319 and 51309213) and the National Key Basic Research Program of China (Grant No. 2014CB046204).

1 Chakrabarti S. Handbook of Offshore Engineering. Amsterdam: Elsevier, 2005
2 Yang M D, Teng B, Xiao L F, et al. Full time-domain nonlinear coupled dynamic analysis of a truss spar and its mooring/riser system in irregular wave. Sci China-Phys Mech Astron, 2014, 57: 152–165
3 Frequencies B. Risk assessment data directory. International Association of Oil and Gas Producers. 2010, Report No. 434-17
4 Gao F P, Cassidy M J. Editorial: Special issue on offshore structure-soil interaction. Theor Appl Mech Lett, 2015, 5: 63
5 Det Norske Veritas. Design of offshore wind turbine structures. DNV-OS-J101. 2010
6 Randolph M F, Gaudin C, Gourvenec S, et al. Recent advances in offshore geotechnics for deep water oil and gas developments. Ocean Eng, 2011, 38: 818–834
7 Randolph M F, Murphy B S. Shaft capacity of driven piles in clay. In: Proceedings of 17th Offshore Technology Conference. Houston, 1985. 1: 371–378
8 Lehane B M, Schneider J A, Xu X. A review of design methods for offshore driven piles in siliceous sand. Technical Report, University of Western Australia. 2005
9 American Petroleum Institute. Geotechnical and foundation design considerations, ANSI/API Recommended Practice 2 GEO First Edition, 2011
10 Randolph M F. Design considerations for offshore piles. In: Proceedings of the Conference on Geotechnical Practice in Offshore Engineering. Austin, 1983. 422–439
11 Randolph M F. Science and empiricism in pile foundation design. Géotechnique, 2003, 53: 847–875
12 Poulos H, Hull T. The role of analytical geomechanics in foundation engineering. Foundation engineering: Current principles and practices. American Society of Civil Engineers. Reston, 1989. 2: 1578–1606
13 Hetenyi M. Beams on Elastic Foundations. Ann Arbor: University of Michigan Press, 1946
14 Poulos H G. Behaviour of laterally loaded piles: I—single piles. J Soil Mech Found Div, 1971, 97: 711–731
15 Randolph M F. The response of flexible piles to lateral loading. Géotechnique, 1981, 31: 247–259
16 Jardine R J, Potts D M, Fourie A B, et al. Studies of the influence of non-linear stress–strain characteristics in soil–structure interaction. Géotechnique, 1986, 36: 377–396
17 Reese L C, Cox W R, Koop F D. Analysis of laterally loaded piles in sand. In: Proceedings of the offshore technology conference. Houston, 1974. 95–105
18 O'Neill M W, Murchison J M. An evaluation of *p-y* relationships in sands. Report to American Petroleum Institute. Houston: University of Houston, 1983
19 Suryasentana S K, Lehane B M. Numerical derivation of CPT-based *p-y* curves for piles in sand. Géotechnique, 2014, 64: 186–194
20 Varun A D, Gazetas G. A simplified model for lateral response of large diameter caisson foundations—linear elastic formulation. Soil Dyna Earthq Eng, 2009, 29: 268–291
21 LeBlanc C, Houlsby G T, Byrne B W. Response of stiff piles in sand to long-term cyclic lateral loading. Géotechnique, 2010, 60: 79–90
22 Doherty P, Gavin K. Laterally loaded monopile design for offshore wind farms. Proc Inst Civil Eng-Energy, 2011, 165: 7–17
23 Bekken L. Lateral behavior of large diameter offshore monopile foundations for wind turbines. Dissertation for the Doctoral Degree. TU Delft: Delft University of Technology, 2009
24 Byrne B W, McAdam R, Burd H J, et al. New design methods for large diameter piles under lateral loading for offshore wind applications. In: Proceedings of 3rd International Symposium on Frontiers in Offshore Geotechnics. Oslo: CRC Press, 2015
25 Gerolymos N, Gazetas G. Winkler model for lateral response of rigid caisson foundations in linear soil. Soil Dyn Earthq Eng, 2006, 26: 347–361
26 Qi W G, Gao F P. Equilibrium scour depth at offshore monopile foundation in combined waves and current. Sci China Tech Sci, 2014, 57: 1030–1039
27 Tao J J, Chen S Y, Su W D. Local reynolds number and thresholds of transition in shear flows. Sci China-Phys Mech Astron, 2013, 56:

263–269
28 Xie X L, Chen Y, Shi Q. Some studies on mechanics of continuous mediums viewed as dfferential manifolds. Sci China-Phys Mech Astron, 2013, 56: 432–456
29 Lin C, Bennett C, Han J, et al. Scour effects on the response of laterally loaded piles considering stress history of sand. Comput Geotech, 2010, 37: 1008–1014
30 Lin C, Han J, Bennett C, et al. Analysis of laterally loaded piles in sand considering scour hole dimensions. J Geotech Geoenviron, 2014, 140: 04014024
31 Qi W G. Scour and liquefaction around a large-diameter monopile and their effects on bearing capacity. Dissertation for Doctoral Degree. Beijing: University of Chinese Academy of Sciences, 2015
32 Qi W G, Gao F P. A modified criterion for wave-induced momentary liquefaction of sandy seabed. Theor Appl Mech Lett, 2015, 5: 20–23
33 Cuéllar P, Mira P, Pastor M, et al. A numerical model for the transient analysis of offshore foundations under cyclic loading. Comput Geotech, 2014, 59: 75–86
34 Wilson D W, Boulanger R W, Kutter B L. Observed seismic lateral resistance of liquefying sand. J Geotech Geoenviron, 2000, 126: 898–906
35 Achmus M, Kuo Y S, Abdel-Rahman K. Behavior of monopile foundations under cyclic lateral load. Comput Geotech, 2009, 36: 725–735
36 Young A G, Remmes B D, Meyer B J. Foundation performance of offshore jack-up drilling rigs. J Geotech Eng, 1984, 7: 841–859
37 Xie Y, Leung C F, Chow Y K. Centrifuge modelling of spudcan-pile interaction in soft clay. Géotechnique, 2012, 62: 799–810
38 Vulpe C, Bienen B, Gaudin C. Predicting the undrained capacity of skirted spudcans under combined loading. Ocean Eng, 2013, 74: 178–188
39 Kohan O, Gaudin C, Cassidy M J, et al. Spudcan extraction from deep embedment in soft clay. Appl Ocean Res, 2014, 48: 126–136
40 Yi J T, Zhao B, Li Y P, et al. Post-installation pore-pressure changes around spudcan and long-term spudcan behaviour in soft clay. Comput Geotech, 2014, 56: 133–147
41 Kong V, Cassidy M J, Gaudin C. Failure mechanisms of a spudcan penetrating next to an existing footprint. Theor Appl Mech Lett, 2015, 5: 64–68
42 ISO. ISO 199051-1: Petroleum and natural gas industries – Site specific assessment of mobile offshore units – Part 1: Jack-ups. Geneva: International Organization for Standardization, 2012
43 Martin C M, Houlsby G T. Combined loading of spudcan foundations on clay: Laboratory tests. Géotechnique, 2000, 50: 325–338
44 Zhang Y, Cassidy M J, Bienen B. A plasticity model for spudcan foundations in soft clay. Can Geotech J, 2014, 51: 629–646
45 Randolph M F, Gourvenec S. Offshore Geotechnical Engineering. New York: Spon Press, 2011
46 Skempton A W. The Bearing Capacity of Clays. London: Building Research Congress, 1951. 1: 180–189
47 Houlsby G T, Martin C M. Undrained bearing capacity factors for conical footings on clay. Géotechnique, 2003, 53: 513–520
48 Hossain M S, Randolph M F. New mechanism-based design approach for spudcan foundations on stiff-over-soft clay. In: Proceedings of Annual Offshore Technology Conference. Houston, 2009. 19907
49 Hossain M S, Randolph M F, Hu Y, et al. Cavity stability and bearing capacity of spudcan foundations on clay. In: The Proceedings of Offshore Technology Conference. Houston, 2006
50 Hossain M S, Randolph M F. Effect of strain rate and strain softening on the penetration resistance of spudcan foundations on clay. Int J Geomech, 2009, 3: 122–132
51 Menzies D, Roper R. Comparison of jackup rig spudcan penetration methods in clay. In: Proceedings of the Offshore Technology Conference. Houston, 2008, 19545
52 Hossain M S, Zheng J, Menzies D, et al. Spudcan penetration analysis for case histories in clay. J Geotech Geoenviron, 2014, 140: 04014034
53 Osborne J J, Houlsby G T, Teh K L, et al. Improved guidelines for the prediction of geotechnical performance of spudcan foundations during installation and removal of jack-up units. In: The Proceedings of the 41st Offshore Technology Conference. Houston, 2009. 20291
54 Lee K K, Randolph M F, Cassidy M J. Bearing capacity on sand overlying clay soils: A simplified conceptual model, Géotechnique, 2013, 63: 1285–1297
55 Hu P, Stanier S A, Cassidy M J, et al. Predicting peak resistance of spudcan penetrating sand overlying clay. J Geotech Geoenviron, 2013, 140: 04013009
56 Qiu G, Grabe J. Numerical investigation of bearing capacity due to spudcan penetration in sand overlying clay. Can Geotech J, 2012, 49: 1393–1407
57 Dean E T R. Predicting Punchthrough of jackup spudcans on sand over clay. Int J Geomech, 2012, 13: 869–876
58 Edwards D H, Potts D M. The bearing capacity of a circular footing under “punch-through” failure. In: Proceedings of 9th International Conference Numerical Modelling in Geomechanics. Ottowa: Taylor & Francis, 2004. 493–498
59 Brown J D, Meyerhof G G. Experimental study of bearing capacity in layered soils. In: Proceedings of 7th International Conference on Soil Mechanics and Foundation Engineering. Mexico, 1969. 97–106
60 Vesic A S. Bearing capacity of shallow foundations. In: Foundation Engineering Handbook. New York: Van Nostrand, 1975, 121–147
61 Merifield R S, Sloan S W, Yu H S. Rigorous plasticity solutions for the bearing capacity of two-layered clays. Géotechnique, 1999, 49: 471–490
62 Romos da Silva M, Smith C C, Jurko J. Squeezing bearing capacity and effects of increasing strength with depth. In: Proceedings of 3rd International Symposium on Frontiers in Offshore Geotechnics. Oslo, 2015. 1299–1304
63 Peire K, Nonneman H, Bosschem E. Gravity base foundations for the thornton bank offshore wind farm. Terra Aqua, 2009, 115: 19–29
64 Prandtl L. Uber die eindringungsfestigkeit plastisher baustoffe und die festigkeit von schneiden. Z Angew Math Mech, 1921, 1: 15–20
65 Terzaghi K. Theoretical Soil Mechanics. New York: Wiley, 1943
66 Brinch Hansen J. A revised and extended formula for bearing capacity. Dan Geotech Inst Bull, 1970, 28: 5–11
67 Meyerhof G G. The bearing capacity of foundations under eccentric and inclined loads. In: Proceedings of 34th International Conference on Soil Mechanics and Foundation Engineering. Zurich, 1953. 440–445
68 Gourvenec S. Shape effects on the capacity of rectangular footings under general loading. Géotechnique, 2007, 57: 637–646
69 Roscoe K H, Schofield A N. The stability of short pier foundations in sand, discussion. Brit Weld J, 1957, 12–18
70 Bransby M F, Randolph M F. Combined loading of skirted foundations. Géotechnique, 1998, 48: 637–655
71 Randolph M F, Puzrin A M. Upper bound limit analysis of circular foundations on clay under general loading. Géotechnique, 2003, 53: 785–796
72 Taiebat H A, Carter J P. Numerical studies of the bearing capacity of shallow foundations on cohesive soil subjected to combined loading. Géotechnique, 2000, 50: 409–418
73 Vulpe C, Gourvenec S, Power M. A generalised failure envelope for undrained capacity of circular shallow foundations under general loading. Géotech Lett, 2014, 4: 187–196
74 Green A P. The plastic yielding of metal junctions due to combined shear and pressure. J Mech Phys Solids, 1954, 2: 197–211
75 Taiebat H A, Carter J P. A failure surface for circular footings on cohesive soils. Géotechnique, 2010, 60: 265–273
76 Bransby M F, Randolph M F. The effect of embedment depth on the undrained reponse of skirted foundations to combined loading. Soils Found, 1999, 39: 19–33
77 Feng X, Gourvenec S, Randolph M F, et al. Effect of a surficial crust on mudmat capacity under fully three-dimensional loading. Geotechnique, 2015, 65: 590–603

78 Feng X, Randolph M F, Gourvenec S, et al. Design approach for rectangular mudmats under fully three-dimensional loading. Géotechnique, 2013, 64: 51–63
79 Gottardi G, Houlsby G T, Butterfield R. Plastic response of circular footings on sand under general planar loading. Géotechnique, 1999, 49: 453–469
80 Houlsby G T, Cassidy M J. A plasticity model for the behaviour of footings on sand under combined loading. Géotechnique, 2002, 52: 117–129
81 Govoni L, Gourvenec S, Gottardi G. A centrifuge study on the effect of embedment on the drained response of shallow foundations under combined loading. Géotechnique, 2011, 61: 1055–1068
82 Dahlberg R. Observations of scour around offshore structures. Can Geotech J, 1983, 20: 617–628
83 Bos K J, Chen Z, Verheij H J, et al. Local scour and protection of F3 offshore GBS platform. In: Proceedings of 21st International Conference on Offshore Mechanics and Arctic Engineering. Oslo: CRC Press, 2002. 219–230
84 Whitehouse R J, Sutherland J, Harris J M. Evaluating scour at marine gravity foundations. In: Proceedings of the ICE-Maritime Engineering, 2011, 164: 143–157
85 Andersen K H, Murff J D, Randolph M F, et al. Suction anchors for deepwater applications. In: Proceedings of the 1st International Symposium on Frontiers in Offshore Geotechnics. Perth: Taylor & Francis Group, 2005. 3–30
86 Erbrich C, Hefer P. Installation of the Laminaria suction piles: A case history. In: Proceedings of Annual Offshore Technology Conference. Houston, 2002. 14240
87 Iskander M, El-Gharbawy S, Olson R. Performance of suction caissons in sand and clay. Can Geotech J, 2002, 39: 576–584
88 Thieken K, Achmus M, Schroer C. On the behavior of suction buckets in sand under tensile loads. Comput Geotech, 2014, 60: 88–100
89 Senders M. Suction caissons in sand as tripod foundations for offshore windturbines. Dissertation for Doctoral Degree. Perth: The University of Western Australia, 2008
90 Gabr M A, Xiao J, Rahman M S. Plastic flow of sand and pullout capacity of suction caissons. J Geotech Geoenviron, 2015, 141: 02815002
91 Andersen K H, Jostad H P. Foundation design of skirted foundations and anchors in clay. In: Proceedings of Annual Offshore Technology Conference. Houston, 1999. 10824
92 Randolph M F. Analysis of suction caisson capacity in clay. In: Proceedings of Annual Offshore Technology Conference. Houston, 2002. 14236
93 Det Norske Veritas. Design and installation of fluke anchors in clay. DNV RP-E301. 2012
94 Neubecker S R, Randolph M F. Profile and frictional capacity of embedded anchor chains. J Geotech Eng, 1995, 121: 797–803
95 Liu H X, Liu C L, Zhao Y B, et al. Reverse catenary equation of the embedded installation line and application to the kinematic model for drag anchors. Appl Ocean Res, 2013, 43: 80–87
96 Cassidy M J, Gaudin C, Randolph M F, et al. A plasticity model to assess the keying of plate anchors. Géotechnique, 2012, 62: 825–836
97 Wang D, Hu Y X, Randolph M F. Keying of rectangular plate anchors in normally consolidated clays. J Geotech Geoenviron, 2011, 137: 1244–1253
98 Tian Y H , Gaudin C, Randolph M F et al. Influence of padeye offset on bearing capacity of three-dimensional plate anchors. Can Geotech J, 2015, 52: 682–693
99 Gaudin C, Tian Y, Cassidy M J, et al. Design and performance of suction embedded plate anchor. In: Proceedings of 3rd International Symposium on Frontiers in Offshore Geotechnics. Oslo: CRC Press, 2015. 863–868
100 Das B M, Shin E C, Dass R N, et al. Suction force below plate anchors in soft clay. Mar Georesour Geotec, 1994, 12: 71–81
101 Yang M, Murf J D, Abuney C P. Undrained capacity of plate anchors under general loading. J Geotech Geoenviron, 2010, 136: 1383–1393
102 Martin C M, Randolph M F. Application of the lower and upper bound theorems of plasticity to collapse of circular foundations. In: Proceedings of 20th Conference Computer Methods in Advanced Geomechanics. Tucson, 2001. 1417–1428
103 Wang D, Hu Y X, Randolph M F. Effect of loading rate on the uplift capacity of plate anchor. In: Proceedings of the 18th Interna-tional Offshore and Polar Engineering Conference. Vancouver, 2008. 727–731
104 Wong P, Gaudin C, Randolph M F, et al. Performance of suction embedded plate anchors in permanent mooring applications. In: Proceedings of the 22th International Offshore and Polar Engineering Conference. Rhode, 2012. 640–645
105 Hu C, Gao F P. Elasto-plasticity and pore-pressure coupled analysis on cyclic loading induced pullout behaviors of a plate anchor. Theor Appl Mech Lett, 2015, 5: 89–92
106 Taiebat H A, Throne C P, Carter J P. Effects of long term loading on storm capacity of vertically loaded anchors. In: Proceedings of 3rd International Symposium on Frontiers in Offshore Geotechnics. Oslo, 2015. 191–196
107 Han C, Wang D, Gaudin C, et al. Soil flow mechanism around deeply embedded plate anchors during monotonic and sustained uplifts. In: Proceedings of 3rd International Symposium on Frontiers in Offshore Geotechnics. Oslo: CRC Press, 2015. 869–874
108 Singh S P, Ramaswamy S V. Influence of frequency on the behaviour of plate anchors subjected to cyclic loading. Mar Georesour Geotec, 2008, 26: 36–50
109 Yu L, Zhou Q, Liu J. Experimental study on the stability of plate anchors in clay under cyclic loading. Theor Appl Mech Lett, 2015, 5: 93–96
110 Andersen K H, Lauritzsen R. Bearing capacity for foundations with cyclic loads. J Geotech Eng, 1988, 114: 540–555
111 Hu C, Gao F P. Numerical modelling of cyclic pullout behaviors of embedded plate anchors in saturated soft clay. In: Proceedings of 33rd International Conference on Ocean, Offshore and Arctic Engineering. San Francisco, 2014. V003T10A025
112 Lieng J T, Kavli A, Hove F, et al. Deep penetrating anchor: Further development, optimization and capacity verification. In: Proceedings of 10th International Offshore & Polar Engineering Conference. Seattle, 2000
113 O'Loughlin C D, Richardson M D, Randolph M F, et al. Penetration of dynamically installed anchors in clay. Géotechnique, 2013, 63: 909–919
114 Wei G, Du H, Xu X H, et al. Experimental investigation of the generation of large-amplitude internal solitary wave and its interaction with a submerged slender body. Sci China-Phys Mech Astron, 2014, 57: 301–310
115 Jeng D S, Seymour B, Gao F P, et al. Ocean waves propagating over a porous seabed: Residual and oscillatory mechanisms. Sci China Series E Technol Sci, 2007, 50: 81–89
116 Wang X L, Li J C. Simulation of triaxial response of granular materials by modified DEM. Sci China-Phys Mech Astron, 2014, 57: 2297–2308
117 Cassidy M, Li J, Hu P, et al. Deterministic and probabilistic advances in the analysis of spudcan behaviour. In: Proceedings of 3rd International Symposium on Frontiers in Offshore Geotechnics. Oslo: CRC Press, 2015. 183–212
118 Li J, Tian Y, Cassidy M J. Failure mechanism and bearing capacity of footings buried at various depths in spatially random soil. J Geotech Geoenviron, 2015, 141: 04014099